PHYSICAL REVIEW E **108**, 014407 (2023)

Effects of noise on the critical points of Turing instability in complex ecosystems

Rui Xiao,[1] Qingyu Gao,[2] Sandro Azaele,[3] and Yongzheng Sun[1,*]
[1]*School of Mathematics, China University of Mining and Technology, Xuzhou 221116, China*
[2]*College of Chemical Engineering, China University of Mining and Technology, Xuzhou 221116, China*
[3]*Department of Physics and Astronomy "G. Galileo," University of Padova, Padova Via Francesco Marzolo 8, 35131 Padova, Italy*

(Received 9 March 2023; accepted 1 July 2023; published 27 July 2023)

Noise is ubiquitous in natural and artificial systems. In a noisy environment, the interactions among nodes may fluctuate randomly, leading to more complicated interactions. In this paper we focus on the effects of noise and network topology on the Turing pattern of ecological networks with activator-inhibitor structure, which may be interpreted as prey-predator interactions. Based on the stability theory of stochastic differential equations, a sufficient condition for the uniform state is derived. The analytical results indicate that noise is beneficial for the uniform state. When the ratio between the diffusion coefficients of the predator and prey increases, the ecosystems can exhibit a transition from a uniform stable state to a Turing pattern, while when the ratio decreases, the ecosystems transit from a Turing pattern to a uniform stable state. There are two crucial critical points in Turing patterns, forward and backward. We find that both forward and backward critical points increase as the noise intensity increases. This means that noise favors a stable homogeneous state compared to a state with a heterogeneous pattern, which is consistent with the analytical results. In addition, noise can weaken the hysteresis phenomenon and even eliminate it in some cases. Furthermore, we report that network topology plays an important role in modulating the uniform state of ecosystems, such as the size of prey-predator systems, the network connectivity, and the strength of interaction.

DOI: 10.1103/PhysRevE.108.014407

I. INTRODUCTION

Reaction-diffusion systems have been widely studied in many fields, such as chemistry, biology, and ecology [1–8]. It was shown that reaction-diffusion systems can exhibit complex self-organized patterns, like stationary dissipative structures [9–11], spiral waves [12,13], or Turing patterns [14,15]. Turing showed that the differences in the diffusion coefficients of activator and inhibitor species could destabilize the uniform stable state and lead to spatially organized patterns [16]. Turing patterns are ubiquitous in real systems; examples include chemical reactions with inhibition [17–19], the process of biological morphogenesis [3,4,20], and ecosystems [21–24]. Specifically, the experimental observation of a sustained nonequilibrium chemical pattern in a single-phase open reactor had been reported [18]. Experiments on zebrafish stripes showed that they arise from a Turing mechanism, and the fish has two kinds of cells that serve the same purposes as an activator and an inhibitor [25]. In prey-predator systems, the prey acts as an activator to increase its population, while the predator acts as an inhibitor to control the population [21].

The dynamic properties of complex-network systems have been the focus of many researchers over the past few decades. In addition, the network topology has an important influence on the dynamics of network systems. For example, the class of scale-free networks can be used to model communications networks and the spreading of computer viruses [26]. May pointed out that the diversity and complexity have a negative correlation with the stability [27]. Since then, many studies have been devoted to the discussion of the relation between the stability and complexity of ecosystems [28–30].

Othmer and Scriven studied the Turing patterns in regular networks and developed a new method for analyzing their instability [31,32]. Subsequently, the effects of network structures on Turing patterns were explored in chemical reactors [33,34]. However, the above studies were limited to small-size regular networks. Nakao and Mikhailov extended the analysis of Turing patterns in regular lattices to the case of large symmetric random networks and proposed a theoretical framework for analyzing the Turing instability in complex networks [35]. Afterward, the studies of Turing patterns on networks attracted much attention and were considered for more complicated networks. For instance, Asllani *et al.* studied the pattern formation on directed networks and found that network topology could make a homogeneous state unstable [36]. The perturbation approach was developed to study Turing patterns in multiplex networks [37]. Turing patterns were studied in multiplex networks, where activator and inhibitor species were put separately in different layers with different network topologies and instability may occur even if two species have the same diffusion coefficients [38]. The theory of Turing instability was applied to reaction-diffusion systems defined on Cartesian networks [39]. Turing patterns on time-varying networks were studied, and the analytical prediction for such instability was obtained [40]. A general theory explaining the influence of network topology on the properties of Turing systems was provided [41]. Siebert *et al.* showed that

---

[*] yzsung@gmail.com

network modularity played an important role in the formation of self-organizing patterns of functional activities [42].

In nature and artificial systems, the dynamic behaviors of complex systems are inevitably influenced by random perturbations [43,44]. It was shown that noise may play an active and constructive role in some collective behaviors. For instance, noisy self-propelled particles with local interactions could be used to explain the phenomenon of self-organized oscillatory motion [45]. Stochastic systems could offer an alternative approach to developing collective robots with robust deterministic behavior [46]. Stochastic Turing patterns have been investigated theoretically [47–51]. Previous studies showed that the parameter regions for stochastic self-organized patterns were larger than in the deterministic case [47,48]. To explore whether stochastic Turing patterns are doable in practice, a synthetic bacterial population was genetically engineered, where the signaling molecules formed a stochastic activator-inhibitor system, and it was found that stochasticity may promote the occurrence of biological patterns [49]. Goldenfeld and co-workers found that the intrinsic noise led to quasipatterns, which could eliminate unphysical fine-tuning or scale separation of Turing models applied to real systems [50]. The persistent intrinsic noise could lead to sustained large-amplitude patterns [51]. However, the influence of noise on the critical points of Turing instability in complex ecological networks is still unknown. Therefore, in this paper we study the effects of noise and network topology on Turing patterns.

We employ ecological networks with prey-predator interactions subject to multiplicative noise and aim to reveal the effects of noise and network topology on the critical points of Turing instability. Based on the stability theory of stochastic differential equations, we derive a sufficient condition for ecosystems to maintain the uniform stable state. The analytical results indicate that noise favors a homogeneous stable state compared to a heterogeneous pattern. Through numerical simulations, we find that the increase in noise intensity can increase both the forward critical point σ_f and the backward critical point σ_b, which means that it helps the ecosystems maintain the uniform stable state while promoting the transition from a Turing pattern to the uniform stable state. The numerical results are consistent with the theoretical analyses. Further, the influence of noise on Turing patterns are also considered in real food-web networks and the results show that noise plays a similar role in modulating Turing patterns. Without the perturbation of noise, the hysteresis phenomenon can be observed and the bifurcation is subcritical. The increase in noise intensity can weaken the hysteresis phenomenon, and even eliminate hysteresis in some cases, and then the bifurcation transforms into supercritical. Further, the network topology has an important influence on Turing patterns. Specifically, a decrease in the size of prey-predator systems, the network connectivity, and the interaction intensity promote homogeneous stable states and facilitate the transition of ecosystems from a Turing pattern to uniform stable states.

The paper is organized as follows. In Sec. II we introduce the network-organized prey-predator systems with multiplicative noise. Section III analyzes the sufficient condition for the uniform stable states of complex ecosystems. In Sec. IV the influence of noise and network topology on the critical points of Turing instability is considered. A summary is given in Sec. V.

II. NETWORK-ORGANIZED PREY-PREDATOR SYSTEMS WITH NOISE

We consider network-organized activator-inhibitor systems with noise perturbation, which can be modeled by the equations

$$\dot{u}_i = f(u_i, v_i) + \varepsilon \sum_{j=1}^{N} a_{ij}(u_j - u_i) + \eta(u_j - u^*)\xi_i(t),$$
$$\dot{v}_i = g(u_i, v_i) + \sigma\varepsilon \sum_{j=1}^{N} a_{ij}(v_j - v_i) + \eta(v_j - v^*)\zeta_i(t), \quad (1)$$

where $i = 1, \dots, N$. As an example of an activator-inhibitor system, the Mimura-Murray prey-predator model is employed as the individual activator-inhibitor dynamics, which is represented by nonlinear functions $f(u, v) = (\frac{a+bu-u^2}{c} - v)u$ and $g(u, v) = u - (1 + dv)v$, in which $u = (u_1, \dots, u_N)^T$ and $v = (v_1, \dots, v_N)^T$ are the densities of prey and predators, respectively. In addition, (u^*, v^*) is the uniform stationary state of the system (1), which implies $f(u^*, v^*) = g(u^*, v^*) = 0$. The uniform stationary state is assumed to be stable in the absence of diffusion and noise perturbation, which requires $f_u + g_v < 0$ and $f_u g_v - f_v g_u > 0$, where $f_u = \partial f/\partial u|_{(u^*,v^*)}$, $f_v = \partial f/\partial v|_{(u^*,v^*)}$, $g_u = \partial g/\partial u|_{(u^*,v^*)}$, and $g_v = \partial g/\partial v|_{(u^*,v^*)}$. The diffusion coefficients of the prey and predator are denoted by ε and $\sigma\varepsilon$, respectively. Generally, the diffusion ratio σ is chosen as the bifurcation parameter, which affects the Turing pattern of the ecosystems. The topology of the network is defined by the matrix $A = (a_{ij})_{N\times N}$. If the nodes i and j are connected, the element $a_{ij} = 1$; otherwise $a_{ij} = 0$ and we assume that $a_{ii} = 0$. The degree of node i is defined as $k_i = \sum_{j=1}^{N} a_{ij}$. Then the Laplacian matrix is $L_{ij} = a_{ij} - k_i\delta_{ij}$, in which δ_{ij} is the Kronecker function. According to the definition of the Laplacian matrix, the diffusion flux of the prey u from node j to node i can be written as $\sum_{j=1}^{N} L_{ij}u_j$, and similarly we have $\sum_{j=1}^{N} L_{ij}v_j$ for the predator v. Here $\xi_i(t)$ and $\zeta_i(t)$ represent standard independent Gaussian white noises, the noise intensity is denoted by η, $\langle\xi_i(t)\rangle = 0$, $\langle\zeta_i(t)\rangle = 0$, $\langle\xi_i(t), \xi_j(t')\rangle = \delta_{ij}\delta(t - t')$, and $\langle\zeta_i(t), \zeta_j(t')\rangle = \delta_{ij}\delta(t - t')$, where δ is the Dirac function. Further, if $\eta = 0$, Eq. (1) degenerates to the deterministic model proposed in [35].

III. THEORETICAL ANALYSES

To explore the effect of noise on the critical points of Turing instability in complex prey-predator systems, we theoretically analyze the model (1) through the stability theory of stochastic differential equations. First, the linear stability analysis is performed. Introducing small perturbations δu_i and δv_i into the uniform state, i.e., $(u_i, v_i) = (u^*, v^*) + (\delta u_i, \delta v_i)$, and substituting the state into Eq. (1), the linearized differential equations for δu_i and δv_i can be obtained

$$\begin{aligned}\delta\dot{u}_i(t) &= f_u\delta u_i + f_v\delta v_i + \varepsilon\sum_{j=1}^{N} a_{ij}(\delta u_j - \delta u_i) + \eta\delta u_i\xi_i(t),\\ \delta\dot{v}_i(t) &= g_u\delta u_i + g_v\delta v_i + \sigma\varepsilon\sum_{j=1}^{N} a_{ij}(\delta v_j - \delta v_i) + \eta\delta v_i\zeta_i(t),\end{aligned} \tag{2}$$

where $f_u = (a + 2bu^* - 3\,u^{*2} - cv^*)/c$, $f_v = -u^*$, $g_u = v^*$, and $g_v = u^* - 1 - 2dv^*$. For simplicity, we suppose that the Gaussian white noises are one dimensional, i.e., $\xi_i(t) = \zeta_i(t) = \xi(t)$. From the mathematical point of view, the one-dimensional Gaussian white noise can be defined as $\xi(t) = \dot{W}(t)$, where $W(t)$ is a one-dimensional standard Brownian motion defined on a complete probability space. Then the disagreement systems (2) can be rewritten in vector form as

$$\begin{aligned}d\delta u &= (f_u\delta u + f_v\delta v)dt + \varepsilon L\delta u dt + \eta\delta u dW(t),\\ d\delta v &= (g_u\delta u + g_v\delta v)dt + \sigma\varepsilon L\delta v dt + \eta\delta v dW(t),\end{aligned} \tag{3}$$

where $\delta u = (\delta u_1, \dots, \delta u_N)^T$ and $\delta v = (\delta v_1, \dots, \delta v_N)^T$ are disagreement vectors and the Laplacian matrix $L = A - K$, where $K = \text{diag}(k_1, \dots, k_N)$. If we let $z = (\delta u, \delta v)^T$, then Eq. (3) becomes

$$dz = (Jz + \tilde{L}z)dt + GzdW(t), \tag{4}$$

where

$$J \triangleq \begin{pmatrix} f_u I_N & f_v I_N \\ g_u I_N & g_v I_N \end{pmatrix}, \quad \tilde{L} \triangleq \begin{pmatrix} \varepsilon L & 0 \\ 0 & \sigma\varepsilon L \end{pmatrix}, \qquad G = \eta I_{2N}.$$

The model (1) maintains the uniform stable state if

$$P(\lim_{t\to\infty}\{|\delta u_i| = 0, |\delta v_i| = 0\}) = 1. \tag{5}$$

In fact, $\lim_{t\to\infty}\{|\delta u_i| = 0, |\delta v_i| = 0\}$ is equal to $\lim_{t\to\infty}|z_i(t)| = 0$, as $z(t) \equiv 0$ is a trivial solution of the disagreement system (4). Therefore, if the trivial solution of Eq. (4) is almost asymptotically stable, that is, $|z(t)| \to 0$ almost holds as $t \to \infty$, then the model (1) can maintain a uniform stable state. In the following, we derive the condition for the model (1) to maintain a uniform stable state. The model (1) can reach a uniform stable state if

$$\gamma \triangleq \lambda_{\max}(J^T + J) + 2\lambda_2(\tilde{L}) - \eta^2 < 0,$$

where $\lambda_{\max}(J^T + J)$ denotes the maximum eigenvalue of matrix $J^T + J$ and $\lambda_2(\tilde{L})$ represents the maximum nonzero eigenvalue of matrix $\tilde{L}$. We prove that if the above inequality is satisfied, the model (1) can remain in the uniform stable state. Applying Itô's formula [52] to the function $V(z) = \ln(z^T z)$ along with the system (4), we have

$$\begin{aligned}V[z(t)] = V[z(0)] &+ \int_0^t \mathcal{L}V[z(s)]ds\\ &+ \int_0^t V_z Gz(s)dW(s), \quad t \geqslant 0,\end{aligned} \tag{6}$$

where

$$\mathcal{L}V(z) = V_z Jz + V_z\tilde{L}z + \tfrac{1}{2}\text{tr}(z^T G^T V_{zz} Gz),$$

and

$$V_z = \frac{2z^T}{z^T z}, \quad V_{zz} = \frac{2I}{z^T z} - \frac{4zz^T}{(z^T z)^2}.$$

Then

$$\mathcal{L}V(z) = \frac{2z^T Jz}{z^T z} + \frac{2z^T\tilde{L}z}{z^T z} + \frac{z^T G^T Gz}{z^T z} - \frac{2(z^T Gz)^2}{(z^T z)^2}. \tag{7}$$

Based on the algebra graph theory, we estimate $\mathcal{L}V(z)$ in Eq. (7). Specifically, since J is an asymmetric matrix, we construct a symmetric matrix $(J^T + J)/2$ so we can obtain

$$\lambda_{\min}\left(\frac{J^T + J}{2}\right) \leqslant \frac{z^T Jz}{z^T z} \leqslant \lambda_{\max}\left(\frac{J^T + J}{2}\right), \tag{8}$$

where $\lambda_{\min}(\cdot)$ and $\lambda_{\max}(\cdot)$ denote the smallest and largest eigenvalues of the matrix, respectively.

As L is a valid symmetric Laplacian matrix, $\tilde{L}$ is also a symmetric matrix according to its definition. Suppose λ_j, $j = 1, \dots, N$, are the eigenvalues of $\tilde{L}$. For $j = 1$, the equation corresponds to a stable manifold ($\lambda_1 = 0$), so we separate it from the others. Thus, we have

$$\lambda_{\min}(\tilde{L}) \leqslant \frac{z^T\tilde{L}z}{z^T z} \leqslant \lambda_2(\tilde{L}). \tag{9}$$

Furthermore, we get

$$\begin{aligned}\frac{z^T Gz}{z^T z} &= \eta,\\ \frac{z^T G^T Gz}{z^T z} &= \frac{z^T G^2 z}{z^T z} = \eta^2.\end{aligned} \tag{10}$$

Substituting Eqs. (8)–(10) into Eq. (7), we obtain the estimation of $\mathcal{L}V(z)$ as

$$\mathcal{L}V[z(t)] \leqslant \lambda_{\max}(J^T + J) + 2\lambda_2(\tilde{L}) - \eta^2, \quad \forall t \geqslant 0. \tag{11}$$

If we let

$$\gamma \triangleq \lambda_{\max}(J^T + J) + 2\lambda_2(\tilde{L}) - \eta^2,$$

then

$$\int_0^t \mathcal{L}V[z(s)]ds \leqslant \gamma t, \quad \forall t \geqslant 0.$$

From Eq. (6) we can obtain

$$\frac{V[z(t)]}{t} \leqslant \frac{V[z(0)]}{t} + \gamma + \frac{\mathcal{M}(t)}{t}, \quad \forall t \geqslant 0,$$

where

$$\mathcal{M}(t) = \int_0^t V_z Gz(s)dW(s) = 2\int_0^t \frac{z^T Gz}{z^T z}dW(s) \tag{12}$$

and $\mathcal{M}(t)$ is a continuous martingale, with $M(0) = 0$. Calculating the quadratic variation of $M(t)$, we have

$$\langle\mathcal{M}(t), \mathcal{M}(t)\rangle = 4\int_0^t \left(\frac{z^T Gz}{z^T z}\right)^2 ds = 4\eta^2 t, \quad \forall t \geqslant 0.$$

Thus,

$$\lim_{t\to+\infty}\frac{\langle\mathcal{M}(t), \mathcal{M}(t)\rangle}{t} < \infty.$$

We apply the strong law of large numbers to obtain

$$\lim_{t\to+\infty}\frac{\mathcal{M}(t)}{t}=0, \quad \text{(a.s.)},$$

where a.s. denotes almost surely. Thus, we get

$$\lim_{t\to+\infty}\sup\frac{V[z(t)]}{t}\leqslant\gamma, \quad \text{(a.s.)}.$$

Consequently,

$$\lim_{t\to+\infty}\sup\frac{\ln\|z(t)\|}{t}\leqslant\frac{\gamma}{2}, \quad \text{(a.s.)}.$$

The solution $z(t)$ of Eq. (4) is almost exponentially convergent to 0 if $\gamma<0$, i.e., $z(t)$ is asymptotically stable. Thus, the model (1) can remain in a stable uniform stationary state when $\gamma<0$. Further, with the increase of noise intensity η, the parameter γ decreases, which means that noise is beneficial for the model (1) to remain in the uniform stable state. Therefore, the theoretical results indicate that noise can promote the ecosystems being in the uniform stable state.

IV. TURING PATTERNS

In this section we conduct numerical simulations on the model (1) to explore the influence of noise and network topology on the Turing patterns in complex prey-predator networks. The stochastic Runge-Kutta algorithm [53] is employed to solve the stochastic differential equations. The order parameter $A(\sigma)=\{\sum_{i=1}^{N}[(u_i-u^*)^2+(v_i-v^*)^2]\}^{1/2}$ is defined to distinguish the patterns in complex ecosystems. It characterizes the difference between the ecosystems' state and the uniform state for a fixed value of σ. Without loss of generality, the parameters chosen in the node dynamics are $a=35$, $b=16$, $c=9$, and $d=\frac{2}{5}$ in the present study, which can keep the ecosystems in a stable uniform state without diffusion and noise perturbation. The fixed point can be calculated as $(u^*,v^*)=(5,10)$.

A. Turing patterns in Erdős-Rényi networks

We begin by studying Turing patterns in Erdős-Rényi networks [54]. Figure 1(a) shows the relationship between the diffusion ratio σ and order parameter $A(\sigma)$ in an Erdős-Rényi network. Therein, in the case of the forward direction, the initial conditions are chosen from the uniform state with small perturbations, while in the backward direction we first evolve a trajectory at a large value of σ and then its final state is used as the initial condition. Increasing the value of σ, we find that $A(\sigma)$ exhibits a discontinuous jump from 0 to a nonzero value at the forward critical point σ_f. Turing instability occurs at σ_f and a stationary Turing pattern has formed. The ecosystems remain in the uniform stable state when $\sigma<\sigma_f$, while the ecosystems are in a Turing pattern when $\sigma\geqslant\sigma_f$. With the decrease of σ, it can be seen that $A(\sigma)$ gradually decreases to zero at σ_b, exhibiting a different path from the forward direction. The ecosystems show a Turing pattern when $\sigma>\sigma_b$, while the ecosystems return to the uniform stable state when $\sigma\leqslant\sigma_b$. In addition, when the value of σ takes values within the range of (σ_b,σ_f), we see that the ecosystems have different patterns for the same parameter value, which is sensitive to the initial conditions. Here the hysteresis phenomenon can be observed.

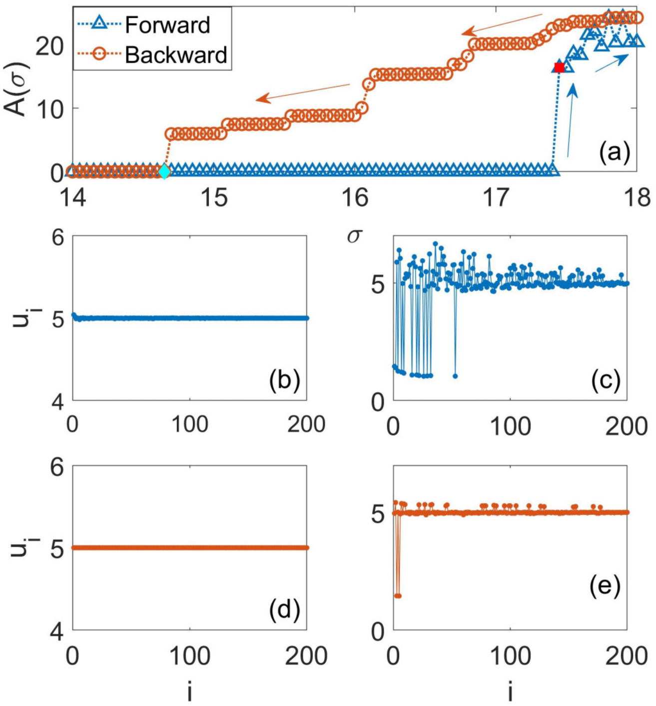

FIG. 1. (a) Relationship between the diffusion ratio σ and the order parameter $A(\sigma)$ in an Erdős-Rényi network in both the forward (blue upper triangles) and the backward (orange circles) directions, in which the forward critical point $\sigma_f=17.45$ and the backward critical point $\sigma_b=14.65$. The parameters are set as network size $N=200$, connection probability $p=0.03$, and noise intensity $\eta=0.2$. The stationary activator pattern is shown for (b) $\sigma=17.40$ (below the forward critical point) and (c) $\sigma=17.50$ (equal to the forward critical point). The stationary activator pattern is shown for (d) $\sigma=14.60$ (below the backward critical point) and (e) $\sigma=14.70$ (above the backward critical point). The nodes are sorted by decreasing order of their degrees.

Figures 1(b) and 1(c) show the stable pattern of prey density before and after the forward critical point, in which the nodes are arranged in descending order of their degrees. In Fig. 1(b) it can be seen that ecosystems are in a uniform stable state, while in Fig. 1(c) ecosystems are in a nonuniform Turing pattern, as some nodes are kicked out of the uniform stable state. Similarly, Figs. 1(d) and 1(e) show the stationary pattern of prey density when σ is below or above the backward critical threshold, and the ecosystems are in a homogeneous stable state and an inhomogeneous Turing pattern, respectively.

The influence of the noise and connection probability of the Erdős-Rényi network on the critical points of Turing instability is shown in Fig. 2. Figures 2(a) and 2(b) show the transition process in the forward direction, and we can see that the forward critical point varies with noise intensity and connection probability. Specifically, Fig. 2(a) illustrates the forward critical points are $\sigma_f\approx 16.50$, 17.10, and 19.40 for $\eta=0.0$, 0.5, and 1.0, respectively. The results indicate that the increased noise intensity causes the forward transition to occur at slightly larger values of σ. Similarly, the forward critical points are $\sigma_f\approx 15.90$, 16.50, and 19.00 in Fig. 2(b).

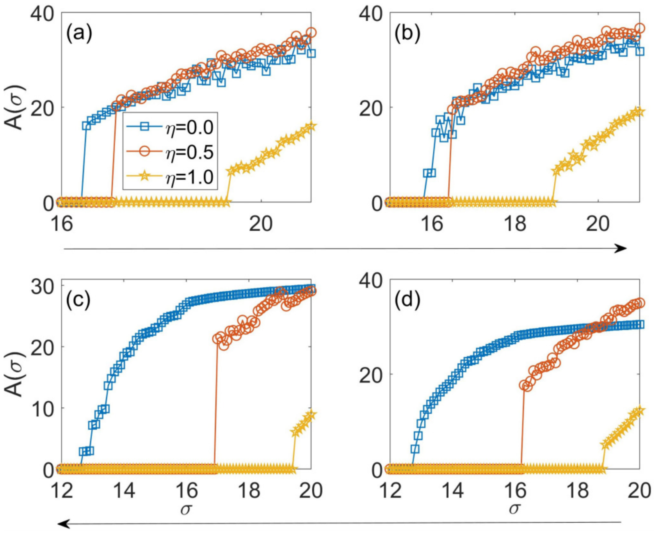

FIG. 2. The order parameter $A(\sigma)$ is plotted versus the increased diffusion ratio σ for different connection probabilities p: (a) $p = 0.04$ and (b) $p = 0.05$. The variation of $A(\sigma)$ with decreasing diffusion ratio is plotted for different values of p: (c) $p = 0.04$ and (d) $p = 0.05$. Three different noise intensities are considered on each graph: $\eta = 0.0$ (blue squares), $\eta = 0.5$ (orange circles), and $\eta = 1.0$ (yellow stars). The other parameters are set as $N = 200$ and $\varepsilon = 0.06$.

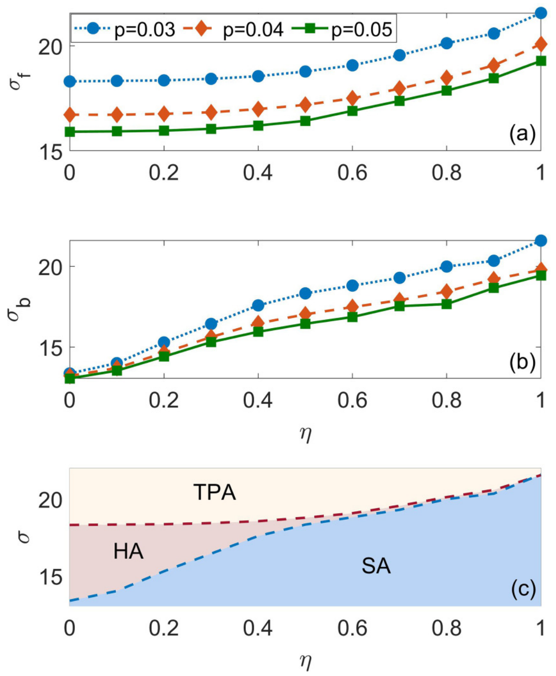

FIG. 3. Average (a) forward and (b) backward critical points σ_f and σ_b, respectively, versus noise intensity across 50 realizations. The connection probability $p = 0.03$ (blue dotted curves), $p = 0.04$ (orange dashed curves), and $p = 0.05$ (green solid curves). (c) Patterns in the parameter plane (σ, η) with $p = 0.03$. The other parameters are $N = 200$ and $\varepsilon = 0.06$.

This means that noise is beneficial for the ecosystems to remain in the homogeneous stable state. Further, the smaller the connection probability, the larger the forward critical point. The reduction of the connection probability helps ecosystems stay in the uniform stable state.

Figures 2(c) and 2(d) present the relationship between $A(\sigma)$ and the reduced diffusion ratio σ when the ecosystems start from a Turing pattern, i.e., the order parameter $A(\sigma) > 0$. In Fig. 2(c) the backward critical points are $\sigma_b \approx 12.60, 16.90$, and 19.40 for $\eta = 0.0$, 0.5, and 1.0, respectively; Fig. 2(d) shows $\sigma_b \approx 12.70$, 16.20, and 18.80. We can see that the increased noise intensity can facilitate the transition of ecosystems from the Turing pattern to the uniform stable state, as it promotes the backward transition that occurs earlier. In addition, the smaller connection probability can increase the backward critical point. Reducing the connection probability can help the ecosystems return to the uniform stable state.

The above results describe the specific transition process of different patterns, in which the forward and backward critical points are important. To proceed, we study the influence of noise on the forward and backward critical points for different connection probabilities; the corresponding results are present in Figs. 3(a) and 3(b). We see that both the forward and backward critical points increase with the increase of noise intensity. In addition, the smaller the connection probability, the larger the forward and backward critical points. The results indicate that the increase in noise intensity and the decrease in connection probability can help ecosystems maintain the uniform and stable state and facilitate the transition from a Turing pattern to the uniform stable state.

To further understand the patterns of the ecosystems, we take $p = 0.03$ as an example to show different patterns in the (σ, η) parameter space in Fig. 3(c). Therein, the orange dotted curve is the forward critical curve and the area above this curve is the Turing pattern area (TPA); when σ is chosen above these critical thresholds, the system is in a Turing pattern. The blue dotted curve represents the backward critical curve and the area below this curve is the uniform stable area (SA); when σ is smaller than these thresholds, the system returns to the uniform stable state. The area enclosed by two curves denotes the hysteresis area (HA), which is known as the coexistence of the uniform stable state and Turing pattern. Without the perturbation of noise, strong hysteresis phenomena can be observed and the Turing bifurcation is subcritical. As the noise intensity increases, the hysteresis effect weakens and may be eliminated in some cases. Specifically, noise can eliminate the hysteresis phenomena and the Turing bifurcation becomes supercritical [55]. With the increase of noise intensity, the SA increases, which means that noise is beneficial for promoting the uniform stable state of ecosystems.

The stability of the ecosystems may be affected in many ways, such as the extinction of existing prey and predators, the interaction cancellation among nodes, and environmental changes. Indeed, these realistic perturbations of ecosystems can be mimicked by the changes of N^2 parameters a_{ij} in the adjacency matrix. For example, the extinction of existing prey and predators can be simulated by removing nodes, the interaction cancellation between nodes can be modeled by deleting existing links, and the environmental changes can be modeled by reducing global link weights between nodes.

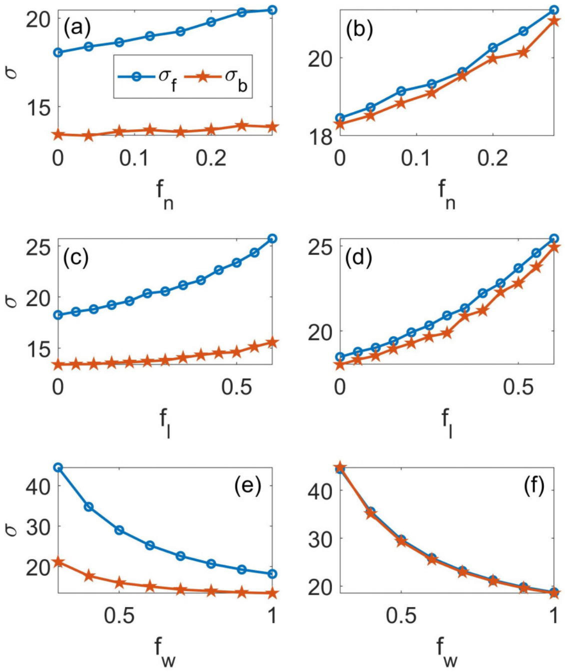

FIG. 4. (a) and (b) Average forward and backward critical points σ_f and σ_b, respectively, versus f_n across 50 realizations. (c) and (d) Critical points σ_f and σ_b characterize the system's response to link perturbation f_l. (e) and (f) Critical points σ_f and σ_b versus f_w. The noise intensity is (a), (c), and (e) $\eta = 0.0$ and (b), (d), and (f) $\eta = 0.5$. The other parameters are $N = 200$, $p = 0.03$, and $\varepsilon = 0.06$.

We study the impact of these three kinds of realistic perturbations on the stability of ecosystems; the results are shown in Fig. 4. First, we randomly remove a fraction f_n of nodes to explore the influence of the extinction of some prey and predators on Turing patterns. Figures 4(a) and 4(b) show the forward critical point σ_f and backward critical point σ_b as a function of node perturbation f_n. We find that with the increase of f_n, both σ_f and σ_b increase. The increase in f_n corresponds to the decrease in the size of prey-predator systems. This indicates that as the size of prey-predator systems decreases, ecosystems are favorable for homogeneous stable states compared to heterogeneous Turing patterns.

Second, we consider the case of randomly deleting a fraction of links f_l, i.e., some of the interactions between nodes disappear. Figures 4(c) and 4(d) show the changes of σ_f and σ_b with link perturbations f_l. We see that as f_l increases, that is, the network connectivity weakens, both critical points σ_f and σ_b increase, which is consistent with the results shown in Figs. 3(a) and 3(b).

Finally, we consider the case where the network structure is fixed but all network weights decrease because of environmental changes. Reducing all network weights to f_ω, we show the variation of σ_f and σ_b as a function of f_w in Figs. 4(e) and 4(f). With the decrease of f_w, both σ_f and σ_b increase. The decrease in network weights means the decrease in the intensity of interactions between nodes, which can promote the ecosystems remaining in the uniform stable state.

It can be concluded that smaller size of prey-predator systems, lower connectivity, and lower interaction strength can facilitate the states being homogeneous rather than heterogeneous. The results are consistent with May's work, in which it was shown that the diversity (the size of prey-predator systems) and complexity (measured by the connectivity and the interaction strength) were not conductive to the stability of ecosystems [27].

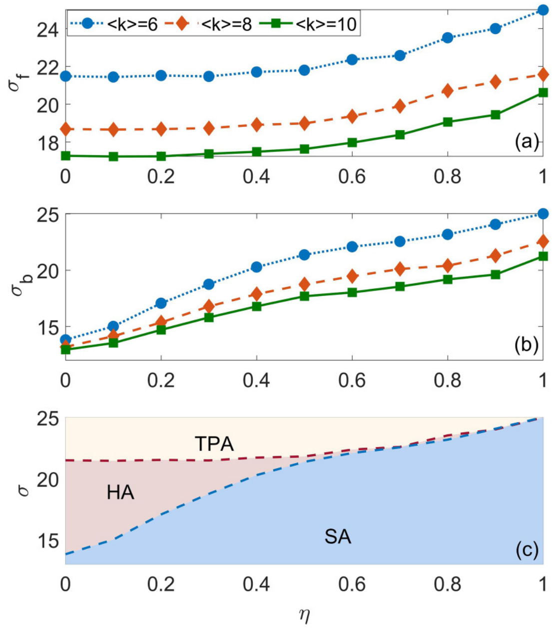

FIG. 5. (a) Effect of noise on the forward critical points σ_f for three mean degrees. (b) Backward critical points σ_b as a function of noise intensity η for 50 realizations. The three different mean degrees are $\langle k \rangle = 6$ (blue dotted curves), $\langle k \rangle = 8$ (orange dashed curves), and $\langle k \rangle = 10$ (green solid curves). (c) Patterns in the parameter plane (σ, η). The description of different areas is the same as in Fig. 3(c). The other parameters are $N = 200$, $\varepsilon = 0.06$, and $\rho = 0.2$.

B. Turing patterns in small-world networks

We investigate the Turing patterns in small-world networks. The small-world network was first proposed by Watts and Strogatz [56]. We consider the nearest-neighbor network first and then reconnect it randomly with probability ρ $(0 < \rho < 1)$, where the small-world network is cable of interpolating between a completely regular network $(\rho = 0)$ and a completely random network $(\rho = 1)$. The influence of noise on the forward and backward critical points for different mean degrees of small-world networks is shown in Figs. 5(a) and 5(b). It can be seen that both the forward and backward critical points increase with the increase of noise intensity. In other words, in the forward direction, noise can promote a homogeneous stable state of ecosystems with small-world network topology, while in the backward direction, noise can help the ecosystems recover from heterogeneous Turing patterns to the uniform stable state. In addition, the smaller the mean degree, the larger the forward and backward critical points, which means that the connectivity of the small-world network can facilitate the ecosystems maintaining the homogeneous stable state and promote the recovery process from a Turing pattern to a homogeneous stable state. Different patterns in the (σ, η) parameter space are shown in Fig. 5(c). It is found that as the noise intensity increases, the hysteresis loop decreases and the

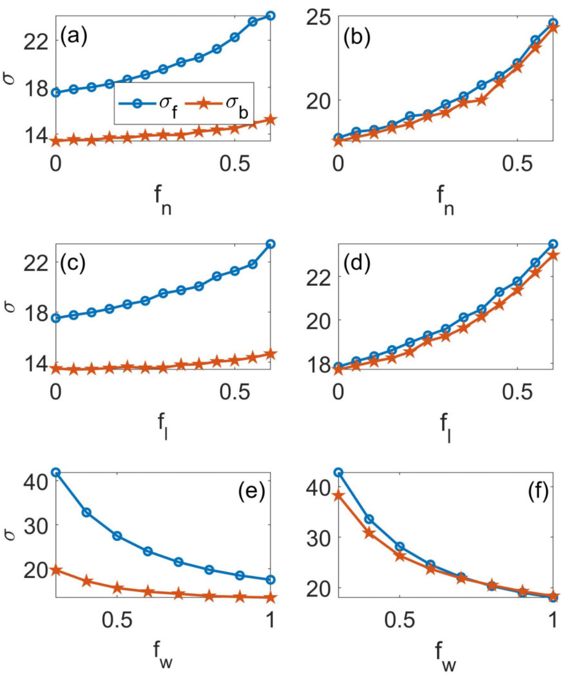

FIG. 6. (a) and (b) Average forward and backward critical points σ_f and σ_b, respectively, versus f_n across 50 realizations. (c) and (d) Critical points σ_f and σ_b characterize the system's response to link perturbation f_l. (e) and (f) Critical points σ_f and σ_b versus f_w. The noise intensity is (a), (c), and (e) $\eta = 0.0$ and (b), (d), and (f) $\eta = 0.5$. The other parameters are $N = 200$, $\langle k \rangle = 10$, and $\varepsilon = 0.06$.

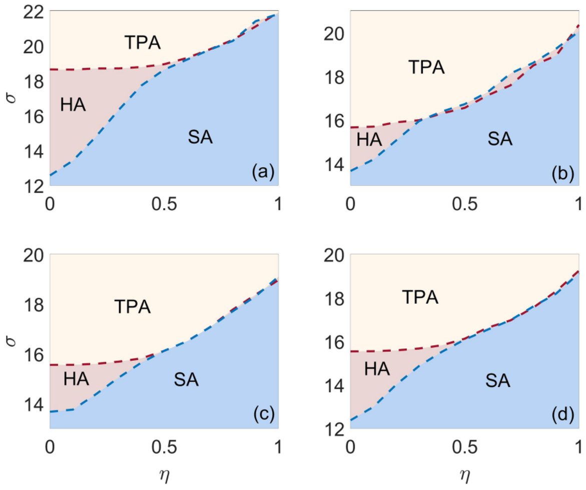

FIG. 7. Dynamics in parameter space (η, σ) for four food-web networks: (a) Michigan, with 39 nodes 39 and 221 links; (b) StMarks, with 54 nodes and 356 links; (c) Everglades, with 69 nodes 69 and 916 links; and (d) Florida, with 128 nodes and 2106 links. The description of different areas is the same as in Fig. 3(c).

SA increases, which indicates that the influence of noise on Turing patterns is similar to that in the Erdős-Rényi network.

In Fig. 6 the effects of three realistic perturbations on the critical points of Turing patterns in small-world networks are considered. Figures 6(a) and 6(b) show the forward (σ_f) and backward (σ_b) critical points versus node perturbations f_n. We can see that with the increase of f_n, both σ_f and σ_b increase. Figures 6(c) and 6(d) plot the critical points σ_f and σ_b as a function of link perturbations f_l. With the increase of f_l, both σ_f and σ_b increase. Figures 6(e) and 6(f) show the relationship between σ_f and σ_b and global perturbations f_w. With the decrease of f_w, σ_f and σ_b increase. The smaller size of prey-predator systems, the lower network connectivity, and the smaller intensity of interaction are favorable for a homogeneous stable state.

C. Turing patterns in real food-web networks

Through the research on Erdős-Rényi and small-world networks, it is concluded that noise can help the ecosystems maintain the homogeneous stable state and promote the ecosystems recovering from a Turing pattern to the uniform stable state. In the following, we explore the effects of noise and network topology on the stability of real food-web networks [57]. We employ the structure of real food-web networks. If nodes i and j have interactions, then $a_{ij} = 1$; otherwise $a_{ij} = 0$, which shows mutualism interactions. Taking four real food-web networks (Michigan, StMarks, Everglades, and Florida) as examples, the influence of noise on the critical points of Turing patterns is shown in Fig. 7. Therein, Michigan represents the lake control network, StMarks represents the river flow network, Everglades represents the graminoid marshes, and Florida represents the bay trophic exchange network. These food-web networks include fishes, mammals, birds, arthropods, plants, etc. It can be seen that with the increase of noise intensity, the TPA and HA decrease, while the SA increases. We can conclude that noise can help the ecosystems maintain a homogeneous stable state in food-web networks and help the ecosystems return to a homogeneous stable state.

Taking the Michigan food-web network as an example, we study the effects of three perturbations on the stability of ecosystems. Figures 8(a) and 8(b) plot the critical points σ_f and σ_b versus node perturbation f_n. We see that with the increase of f_n, σ_f and σ_b increase and noise can help σ_b increases faster, resulting in a decreased HA. Figures 8(c) and 8(d) show the change of critical points σ_f and σ_b with link perturbation f_l. In Fig. 8(c), with the increase of f_l, σ_f increases slightly at first and rapidly, while σ_b changes steadily. In Fig. 8(d) both σ_f and σ_b increase steadily at small f_l and then become faster. Figures 8(e) and 8(f) show the critical points σ_f and σ_b as a function of f_w. With the decrease of f_w, σ_f and σ_b increase. The influence of noise and network topology on Turing patterns is similar to that in Erdős-Rényi and small-world networks.

V. CONCLUSION

We have investigated the influence of noise and network topology on the critical points of Turing instability in complex prey-predator networks. Based on the stability theory of stochastic differential equations, a sufficient condition for the uniform stable state of ecosystems was derived. The analytical results indicated that noise is beneficial for the uniform states. The diffusion ratio σ was chosen as the bifurcation parameter. With the increase of σ, the ecosystems exhibited the transition from a homogeneous stable state to a Turing

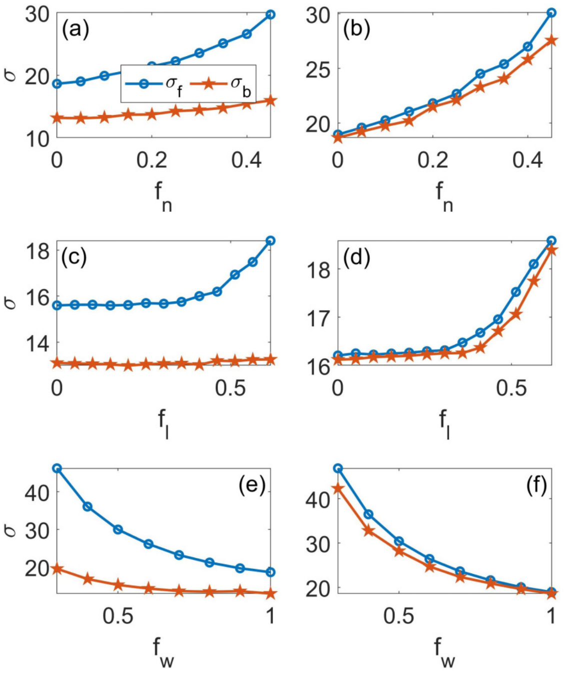

FIG. 8. (a) and (b) Average forward and backward critical points σ_f and σ_b, respectively, versus f_n across 50 realizations. (c) and (d) Critical points σ_f and σ_b characterize the system's response to link perturbation f_l. (e) and (f) Critical points σ_f and σ_b versus f_w. The noise intensity is (a), (c), and (e) $\eta = 0.0$ and (b), (d), and (f) $\eta = 0.5$. The network topology is chosen to be that of Michigan.

pattern, while as σ decreased, the ecosystems transited from a Turing pattern to a uniform stable state. It is worth noting that the forward critical point σ_f and the backward critical point σ_b increased with the noise intensity. This implies that noise can promote the ecosystems maintaining the uniform stable state and facilitate the return from a Turing pattern to a stable state, which is consistent with the analytical results. The influence of noise on Turing patterns was also studied in real food-web networks; the results were similar to those in Erdős-Rényi and small-world networks. According to Refs. [58,59], the real food-web network is a non-normal network, in which its adjacency matrix is referred to as non-normal. However, the theoretical analyses of Turing patterns on a non-normal network are different from analyses of the symmetry network [58,59], which needs to be studied in the future.

Without the perturbation of noise, hysteresis phenomena could be observed and the Turing bifurcation was subcritical. As the noise intensity increased, the hysteresis effect weakened and could be eliminated in some cases, that is, noise could eliminate the hysteresis phenomena and the Turing bifurcation became supercritical. Closing the hysteresis area is meaningful as one could clarify and explain the formation of the patterns.

We found that network topology has important effects on the critical points of Turing patterns, including the size of prey and predator systems, the connectivity, and the interaction strength. We have shown that the smaller size of prey-predator systems, lower connectivity, and smaller interaction strength can facilitate the states being homogeneous and stable rather than being in heterogeneous Turing patterns. The results are consistent with May's work, in which he showed that the diversity (the size of prey-predator systems) and complexity (measured by the connectivity and the interaction strength) was not conductive to the stability of ecosystems.

ACKNOWLEDGMENTS

This work was supported by the National Natural Science Foundation of China (Grants No. 12271519 and No. 2211001016), the Natural Science Foundation of Jiangsu Province (Grants No. BK20221107 and No. BK20211241), and the Fundamental Research Funds for the Central Universities (Grant No. 2022QN1091). Postdoctoral Science Foundation of China (Grants No. 2017M621860 and No. 2019T120476).

---

[1] Q. Ouyang and H. L. Swinney, Nature (London) **352**, 610 (1991).
[2] I. Lengyel and I. R. Epstein, Proc. Natl. Acad. Sci. USA **89**, 3977 (1992).
[3] H. Meinhardt and A. Gierer, Bioessays **22**, 753 (2000).
[4] P. K. Maini, R. E. Baker, and C.-M. Chuong, Science **314**, 1397 (2006).
[5] M. Rietkerk and J. van de Koppel, Trends Ecol. Evol. **23**, 169 (2008).
[6] Q.-X. Liu, A. Doelman, V. Rottschäfer, M. de Jager, P. M. Herman, M. Rietkerk, and J. van de Koppel, Proc. Natl. Acad. Sci. USA **110**, 11905 (2013).
[7] G. Giunta, H. Seyed-Allaei, and U. Gerland, Commun. Phys. **3**, 167 (2020).
[8] P. Clusella, M. C. Miguel, and R. Pastor-Satorras, Commun. Phys. **4**, 13 (2021).
[9] K. Agladze, V. Krinsky, and A. Pertsov, Nature (London) **308**, 834 (1984).
[10] L. A. Lugiato and R. Lefever, Phys. Rev. Lett. **58**, 2209 (1987).
[11] M. Tlidi, M. Taki, and T. Kolokolnikov, Chaos **17**, 037101 (2007).
[12] D. Barkley, Phys. Rev. Lett. **72**, 164 (1994).
[13] S.-i. Shima and Y. Kuramoto, Phys. Rev. E **69**, 036213 (2004).
[14] V. K. Vanag and I. R. Epstein, Science **294**, 835 (2001).
[15] V. A. Vasiliev, in *Thermodynamics of Biological Processes*, edited by I. Lamprecht and A. I. Zotin (Walter de Gruyter, Berlin, 1978), pp. 277–292.
[16] A. M. Turing, Philos. Trans. R. Soc. London Ser. B **237**, 37 (1952).
[17] I. Prigogine and R. Lefever, J. Chem. Phys. **48**, 1695 (1968).
[18] V. Castets, E. Dulos, J. Boissonade, and P. De Kepper, Phys. Rev. Lett. **64**, 2953 (1990).
[19] O. E. Shklyaev, V. V. Yashin, S. I. Stupp, and A. C. Balazs, Commun. Phys. **3**, 70 (2020).
[20] M. P. Harris, S. Williamson, J. F. Fallon, H. Meinhardt, and R. O. Prum, Proc. Natl. Acad. Sci. USA **102**, 11734 (2005).
[21] M. Mimura and J. Murray, J. Theor. Biol. **75**, 249 (1978).
[22] J. L. Maron and S. Harrison, Science **278**, 1619 (1997).

[23] M. Baurmann, T. Gross, and U. Feudel, J. Theor. Biol. **245**, 220 (2007).

[24] E. Pigani, D. Sgarbossa, S. Suweis, A. Maritan, and S. Azaele, Proc. Natl. Acad. Sci. USA **119**, e2211449119 (2022).

[25] S. Miyazawa, M. Okamoto, and S. Kondo, Nat. Commun. **1**, 66 (2010).

[26] R. Pastor-Satorras and A. Vespignani, Phys. Rev. Lett. **86**, 3200 (2001).

[27] R. M. May, Nature (London) **238**, 413 (1972).

[28] K. S. McCann, Nature (London) **405**, 228 (2000).

[29] A. R. Ives and S. R. Carpenter, Science **317**, 58 (2007).

[30] D. Gravel, F. Massol, and M. A. Leibold, Nat. Commun. **7**, 12457 (2016).

[31] H. G. Othmer and L. Scriven, J. Theor. Biol. **32**, 507 (1971).

[32] H. G. Othmer and L. Scriven, J. Theor. Biol. **43**, 83 (1974).

[33] W. Horsthemke, K. Lam, and P. K. Moore, Phys. Lett. A **328**, 444 (2004).

[34] P. K. Moore and W. Horsthemke, Physica D **206**, 121 (2005).

[35] H. Nakao and A. S. Mikhailov, Nat. Phys. **6**, 544 (2010).

[36] M. Asllani, J. D. Challenger, F. S. Pavone, L. Sacconi, and D. Fanelli, Nat. Commun. **5**, 4517 (2014).

[37] M. Asllani, D. M. Busiello, T. Carletti, D. Fanelli, and G. Planchon, Phys. Rev. E **90**, 042814 (2014).

[38] N. E. Kouvaris, S. Hata, and A. Díaz-Guilera, Sci. Rep. **5**, 10840 (2015).

[39] M. Asllani, D. M. Busiello, T. Carletti, D. Fanelli, and G. Planchon, Sci. Rep. **5**, 12927 (2015).

[40] J. Petit, B. Lauwens, D. Fanelli, and T. Carletti, Phys. Rev. Lett. **119**, 148301 (2017).

[41] X. Diego, L. Marcon, P. Müller, and J. Sharpe, Phys. Rev. X **8**, 021071 (2018).

[42] B. A. Siebert, C. L. Hall, J. P. Gleeson, and M. Asllani, Phys. Rev. E **102**, 052306 (2020).

[43] Y. Meng, Y.-C. Lai, and C. Grebogi, J. R. Soc. Interface. **17**, 20200645 (2020).

[44] X. Tian, H. Goetz, A. Stone, R. Zhang, and Y.-C. Lai, Biophys. J. **121**, 126a (2022).

[45] C. Chen, S. Liu, X.-q. Shi, H. Chaté, and Y. Wu, Nature (London) **542**, 210 (2017).

[46] S. Li, R. Batra, D. Brown, H.-D. Chang, N. Ranganathan, C. Hoberman, D. Rus, and H. Lipson, Nature (London) **567**, 361 (2019).

[47] T. Biancalani, D. Fanelli, and F. Di Patti, Phys. Rev. E **81**, 046215 (2010).

[48] M. Asllani, T. Biancalani, D. Fanelli, and A. J. McKane, Eur. Phys. J. B **86**, 476 (2013).

[49] D. Karig, K. M. Martini, T. Lu, N. A. DeLateur, N. Goldenfeld, and R. Weiss, Proc. Natl. Acad. Sci. USA **115**, 6572 (2018).

[50] T. Butler and N. Goldenfeld, Phys. Rev. E **84**, 011112 (2011).

[51] T. Biancalani, F. Jafarpour, and N. Goldenfeld, Phys. Rev. Lett. **118**, 018101 (2017).

[52] L. Arnold, *Stochastic Differential Equations* (Springer, New York, 1974).

[53] R. L. Honeycutt, Phys. Rev. A **45**, 600 (1992).

[54] P. Erdős and A. Rényi, Publ. Math. Inst. Hung. Acad. Sci. **5**, 17 (1960).

[55] S. Hata, H. Nakao, and A. S. Mikhailov, Europhys. Lett. **98**, 64004 (2012).

[56] D. J. Watts and S. H. Strogatz, Nature (London) **393**, 440 (1998).

[57] http://vlado.fmf.uni-lj.si/pub/networks/data/bio/foodweb/foodweb.htm.

[58] M. Asllani, R. Lambiotte, and T. Carletti, Sci. Adv. **4**, eaau9403 (2018).

[59] R. Muolo, M. Asllani, D. Fanelli, P. K. Maini, and T. Carletti, J. Theor. Biol. **480**, 81 (2019).